

Local and remote controls on observed Arctic warming

J. A. Screen,¹ C. Deser,² and I. Simmonds¹

Received 4 March 2012; revised 17 April 2012; accepted 22 April 2012; published 30 May 2012.

[1] The Arctic is warming two to four times faster than the global average. Debate continues on the relative roles of local factors, such as sea ice reductions, versus remote factors in driving, or amplifying, Arctic warming. This study examines the vertical profile and seasonality of observed tropospheric warming, and addresses its causes using atmospheric general circulation model simulations. The simulations enable the isolation and quantification of the role of three controlling factors of Arctic warming: 1) observed Arctic sea ice concentration (SIC) and sea surface temperature (SST) changes; 2) observed remote SST changes; and 3) direct radiative forcing (DRF) due to observed changes in greenhouse gases, ozone, aerosols, and solar output. Local SIC and SST changes explain a large portion of the observed Arctic near-surface warming, whereas remote SST changes explain the majority of observed warming aloft. DRF has primarily contributed to Arctic tropospheric warming in summer. **Citation:** Screen, J. A., C. Deser, and I. Simmonds (2012), Local and remote controls on observed Arctic warming, *Geophys. Res. Lett.*, 39, L10709, doi:10.1029/2012GL051598.

1. Introduction

[2] Surface temperatures are rising faster in the Arctic than over the globe as a whole [*Intergovernmental Panel on Climate Change*, 2007], a phenomenon commonly known as Arctic amplification (AA). There has been much discussion about the causes of observed AA [e.g., *Serreze and Francis*, 2006; *Graversen et al.*, 2008; *Serreze et al.*, 2009; *Screen and Simmonds*, 2010a, 2010b; *Serreze and Barry*, 2011; *Bintanja et al.*, 2011].

[3] One key aspect of this debate has been the vertical profile of Arctic warming and its interpretation in the context of the causes of AA. It has been shown that the vertical structure of Arctic warming can provide insight into its underlying causes, because different driving mechanisms may have a different “fingerprint” in the atmospheric column. Sea ice concentration (SIC) or sea surface temperature (SST) changes are understood to induce a temperature response that is strongest in the lowermost atmosphere [*Serreze et al.*, 2009; *Deser et al.*, 2010; *Kumar et al.*, 2010; *Screen and Simmonds*, 2010a, 2010b; *Sedláček et al.*, 2012; *Orsolini et al.*, 2012] whereas changes in atmosphere energy transport may cause a maximum thermal response in the

mid-troposphere [*Alexeev et al.*, 2005; *Graversen et al.*, 2008; *Yang et al.*, 2010; *Chung and Räisänen*, 2011].

[4] A number of studies have examined the vertical profile of recent Arctic warming based on atmospheric reanalyses [*Graversen et al.*, 2008; *Screen and Simmonds*, 2010a, 2010b; *Alexeev et al.*, 2012]. On the basis of the ERA-40 reanalysis, *Graversen et al.* [2008] found greater warming aloft than at the surface over the period 1979–2001, which led them to conclude that atmospheric poleward energy transport, not Arctic sea ice loss, was the main driver of AA. In contrast, alternative reanalysis data sets analysed by *Serreze et al.* [2009] and *Screen and Simmonds* [2010a] showed strongest AA at the surface, consistent with changes in the surface energy budget due to sea ice loss [*Screen and Simmonds*, 2010b]. This discrepancy can be explained by two compounding factors: errors in ERA-40 that result in exaggerated warming in the mid- to lower-troposphere [*Screen and Simmonds*, 2011; *Alexeev et al.*, 2012], and an increase in the rate of sea ice decline [*Comiso et al.*, 2008], that has strengthened surface-based AA over the past decade [*Serreze et al.*, 2009; *Screen and Simmonds*, 2010a].

[5] Despite differing perspectives on the relative role of Arctic sea ice loss in AA, both *Graversen et al.* [2008] and *Screen and Simmonds* [2010a] found mid-tropospheric Arctic warming in all seasons, which, as mentioned above, is highly suggestive of horizontal energy transport changes as opposed to surface energy budget changes. Thus, it appears very likely that multiple processes are important for observed AA (see review by *Serreze and Barry* [2011]). Furthermore, these multiple mechanisms of AA are likely to be inter-connected, which makes them hard to disentangle using observations (or reanalyses) alone. For example, increased poleward heat transport would likely enhance sea ice melt and therefore, trigger surface-based AA [*Graversen et al.*, 2011; *Chung and Räisänen*, 2011].

[6] The seasonality of Arctic warming may also provide clues as to relative importance of the multiple driving processes [*Lu and Cai*, 2009]. The air temperature response to Arctic sea ice loss is understood to be largest in autumn and early winter [*Deser et al.*, 2010]. The strong temperature inversion amplifies near-surface polar warming primarily in winter [*Deser et al.*, 2010; *Bintanja et al.*, 2011]. *Chung and Räisänen* [2011] argue that the strength and vertical structure of summertime Arctic warming is a good indicator of how much climate forcing from lower latitudes contributes to Arctic warming.

[7] In this study we revisit the vertical profile and seasonality of observed Arctic warming and seek to quantify the forcings that are responsible for it. In this context, the terminology “forcings” is used to describe both external forcings, such as changes in greenhouse gases or aerosols, and atmospheric lower boundary forcings, such as changes in SST and SIC. We utilise atmospheric general circulation model (AGCM) hind-casts to isolate and quantify the role of

¹School of Earth Sciences, University of Melbourne, Melbourne, Victoria, Australia.

²Global and Climate Dynamics, National Center for Atmospheric Research, Boulder, Colorado, USA.

Corresponding author: J. A. Screen, School of Earth Sciences, University of Melbourne, Melbourne, Vic 3010, Australia. (screenj@unimelb.edu.au)

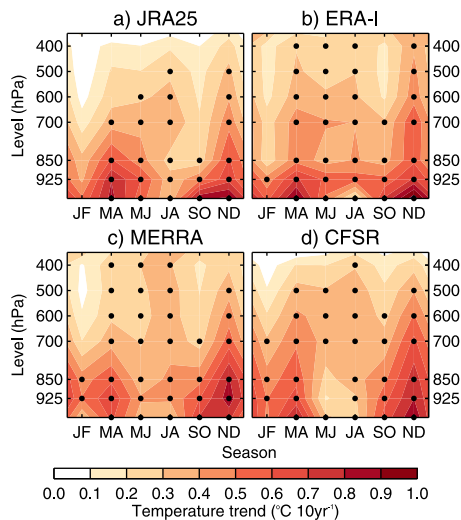


Figure 1. Vertical and seasonal structure of Arctic-mean temperature trends (1979–2008) in the (a) JRA25, (b) ERA-I, (c) MERRA and (d) CFSR reanalyses, respectively. Black dots show trends that are statistically significant at the 95% level ($p < 0.05$) based on a two-tailed student's t -test.

three forcing factors to recent Arctic warming: 1) observed Arctic SIC and SST changes; 2) observed remote SST changes; and 3) direct radiative forcing (DRF) due to observed changes in greenhouse gases, ozone, sulphate and volcanic aerosols, and solar output. These simulations add new insight into the physical processes underlying the observed Arctic warming. A major advance in our study is the use of specially-designed model simulations to quantify the relative roles of local and remote forcing of observed Arctic warming, expanding on previous studies that have shown qualitative differences in the vertical profile and seasonality of Arctic warming in response to these factors.

2. Data and Methods

2.1. Model Simulations

[8] We utilize two independent AGCMs: the NCAR Community Atmosphere Model version 3 (CAM3) and the UK-Australian Unified Model version 7.3 (UM7.3). CAM3 is the atmospheric component of the NCAR Community Climate System Model version 3 (CCSM3), which participated in the third Coupled Model Intercomparison Project (CMIP). The version used here has 26 vertical levels and a spectral resolution of T42, roughly equivalent to 2.8 degrees of latitude and longitude. UM7.3 has been developed by the UK Meteorological Office Hadley Centre and is the atmospheric model used in their Global Environmental Model version 2 (HadGEM2) and in the Australian Community Climate and Earth System Simulator (ACCESS) version 1.0. Both HadGEM2 and ACCESS are participating models in the fifth CMIP. The configuration of UM7.3 used here has 38 vertical levels with a horizontal resolution of 1.25 degrees of latitude by 1.875 degrees of longitude. For further details the reader is directed to *Collins et al.* [2006] and *Martin et al.* [2011], for CAM3 and UM7.3 respectively.

[9] Two distinct experiments have been performed identically with each model. In both experiments, the AGCMs were coupled to a land surface model and the land surface

boundary conditions were free to evolve. The oceanic surface boundary conditions were prescribed. In the first experiment, the models were forced with the observed evolution of monthly SIC and SST globally for the period 1979–2008, from the *Hurrell et al.* [2008] data set. Hereafter we will refer to this as the GLB experiment.

[10] In the second experiment, the models were forced with the observed evolution of monthly Arctic SIC. SSTs were allowed to vary from year-to-year only in regions of Arctic sea ice change, to account for local SST modifications related *directly* to sea ice change, but were specified as the climatological annual cycle elsewhere. Hereafter we will refer to this as the ARC experiment. In both GLB and ARC, greenhouse gas concentrations, ozone, sulphate and volcanic aerosols, and solar output were all held constant.

[11] A third experiment has been performed in CAM3 only. In this experiment the oceanic surface boundary conditions were prescribed as in GLB, but additionally the model was forced with the observed evolution of greenhouse gases, ozone, sulphate and volcanic aerosols, and solar output. These forcings were taken from *Meehl et al.* [2006] and are based on observations until the year 2000 and the Special Report on Emissions Scenarios (SRES) A1B scenario from 2000 to 2008. As explained by *Deser and Phillips* [2009] and originally by *Folland et al.* [1998], this approach does not “double count” the atmospheric radiative forcing because only the direct effect is specified, whereas the indirect effect (via changes in SST and SIC) is included in the prescribed surface forcing. Hereafter we will refer to this as the ALL experiment.

[12] The simulations cover the 30-year period from 1979 to 2008. To quantify the effects of atmospheric intrinsic variability (AIV), all three experiments were conducted multiple times starting from different atmospheric initial conditions. Both GLB and ARC were run five times in CAM3 and eight times in UM7.3, giving an ensemble of thirteen simulations. ALL was performed five times using CAM3. The thermal responses in GLB and ARC were highly consistent between the two independent AGCMs and therefore we only present the ensemble-mean of all thirteen simulations in what follows. We analyse temperature fields at the surface and on seven standard pressure levels (925, 850, 700, 600, 500, 400, 300 hPa).

2.2. Reanalyses

[13] We use temperature fields from four of the latest atmospheric reanalyses: the Japanese 25-year reanalysis (JRA25) [*Onogi et al.*, 2007], ECMWF ERA-Interim reanalysis (ERA-I) [*Dee et al.*, 2011], NASA Modern-Era Retrospective analysis for Research and Applications (MERRA) [*Rienecker et al.*, 2011] and the NCEP Climate Forecast System Reanalysis (CFSR) [*Saha et al.*, 2010]. For the sake of comparison (and to facilitate averaging across the reanalyses), all reanalysis temperature fields were re-gridded on to a 2.5 degree latitude-longitude grid, at the surface and on the same seven vertical levels as the model output.

[14] Figure 1 shows the vertical and seasonal structure of Arctic-mean temperature trends over the 30-year period from 1979 to 2008 in the four reanalyses. Here and in what follows the Arctic is defined as the region poleward of 67°N (results were comparable for other reasonable definitions of the Arctic, e.g., >60, 65, 70°N), which comprises of approximately 65% ocean and 35% land by area. The “seasons” are

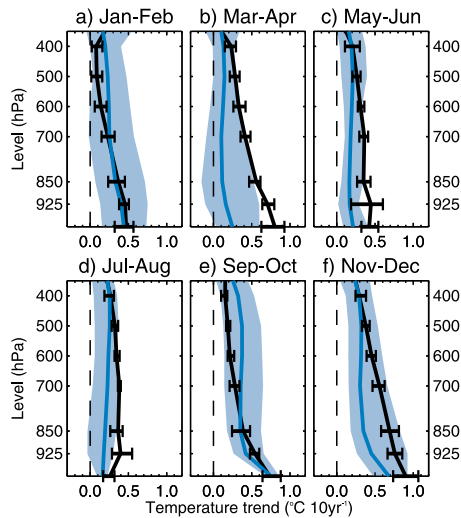


Figure 2. Vertical profile of Arctic-mean temperature trends (1979–2008) for (a) Jan–Feb, (b) Mar–Apr, (c) May–Jun, (d) Jul–Aug, (e) Sep–Oct, and (f) Nov–Dec. The black lines denote the reanalysis ensemble-mean trends and the whiskers show the reanalysis ensemble spread. The blue lines denote the model ensemble-mean trends from the GLB experiment and the shaded envelopes show the model ensemble spread.

defined as January–February (JF), March–April (MA), May–June (MJ), July–August (JA), September–October (SO), and November–December (ND). We have chosen to conduct our analyses on these six two-month “seasons” rather than the conventional four (following *Deser et al.* [2010]) because the thermal response to Arctic sea ice loss displays rapid monthly changes, which tend to be blurred out if three-month averages are employed.

[15] Although the Arctic-mean temperature trends are not identical, the four reanalyses do, however, depict a consistent vertical and seasonal pattern of warming (Figure 1). The strong agreement between the reanalyses, in spite of differences in the observations assimilated, data assimilation techniques and underpinning reanalysis model physics, lends credence to the veracity of the trends. Further, *Screen and Simmonds* [2011] showed that, barring one clearly erroneous reanalysis not used here (ERA-40), the current breed of reanalyses can accurately (to within the 95% confidence level) reproduce Arctic-mean upper-air temperature trends measured by radiosondes and satellites.

3. Analysis and Results

[16] Our first consideration is to determine whether the models depict a realistic climatological-mean seasonal cycle and vertical profile of Arctic-mean temperature. Figure S1 in the auxiliary material shows that the models represent well the main aspects of the seasonal and vertical structure of Arctic temperature found in the reanalyses.¹ Importantly, the models capture the climatological-mean near-surface temperature inversion in the winter months (November–April). However, both UM7.3 and CAM3 simulate overly strong

wintertime temperature inversions. This problem is common to many climate models [*Medeiros et al.*, 2011; *Zhang et al.*, 2011]. The implications of these model biases will be discussed later and we are mindful of this issue as we proceed.

[17] Next we address whether the AGCM simulations can capture the seasonal and vertical structure of Arctic warming found in the reanalyses. Figure 2 shows, for each season, the vertical profile of Arctic temperature trends averaged across the four reanalyses (hereafter termed OBS) in black and the GLB ensemble-mean in blue. The spread of the four reanalyses (the range between minimum and maximum; whiskers in Figure 2) allows a quantitative assessment of uncertainty in Arctic temperature trends due to differences in the reanalysis process and different background atmospheric states. The model ensemble spread (the range between minimum and maximum of the thirteen individual simulations; shaded envelope in Figure 2) provides an estimate of the uncertainty due to AIV and, to a lesser extent, model differences. The model ensemble spread is generally larger than the reanalysis ensemble spread.

[18] The vertical profiles of the temperature trends are in broad agreement between OBS and the GLB ensemble-mean. Of course, perfect agreement should not be expected since the OBS trends will contain the imprint of AIV, which is averaged out, at least partially, in the GLB ensemble-mean. In most seasons and at the majority of heights in the atmosphere, the OBS trends lie within the spread of the individual GLB ensemble members. When the reanalysis uncertainty is also taken into account, there are only two trends that differ significantly between GLB and OBS (in the sense that there is no overlap between the model ensemble spread and reanalysis ensemble spread): the GLB simulations underestimate the surface and 925 hPa warming during MA (Figure 2b). This discrepancy is most pronounced over the terrestrial portion of our Arctic domain (not shown). The observed springtime terrestrial Arctic warming has been attributed in part to decreases in snow cover extent [*Déry and Brown*, 2007], which are not specified in our simulations and therefore, may in part explain the stronger land surface warming in OBS compared to GLB. In ND, the GLB ensemble-mean shows weaker warming at 925 and 850 hPa than OBS. A possible explanation for this discrepancy is that the climatological near-surface temperature inversion is stronger in the models than it is in the reanalyses. Both models overestimate the strength of the climatological-mean temperature inversion in ND, JF and MA (Figure S1), which may excessively confine warming to the near-surface layers in the simulations in these seasons. These differences aside, the GLB simulations represent well the seasonality and vertical profile of Arctic warming in OBS.

[19] Figures 3a and 3b show the vertical and seasonal structure of Arctic temperature trends in OBS and the GLB ensemble mean, respectively. Both depict warming throughout the troposphere and in all seasons. However, the warming is far from uniform with respect to season or altitude. In both OBS and GLB, there is more pronounced warming in September–February than in May–August. The warming is strongly surface-intensified in SO and ND whereas there is comparatively vertically-uniform warming in MJ and JA. The most obvious discrepancies between OBS and GLB are the larger near-surface warming during MA found in OBS and the larger lower-tropospheric (925–700 hPa) warming during ND in OBS than in GLB. As discussed above, these

¹Auxiliary materials are available in the HTML. doi:10.1029/2012GL051598.

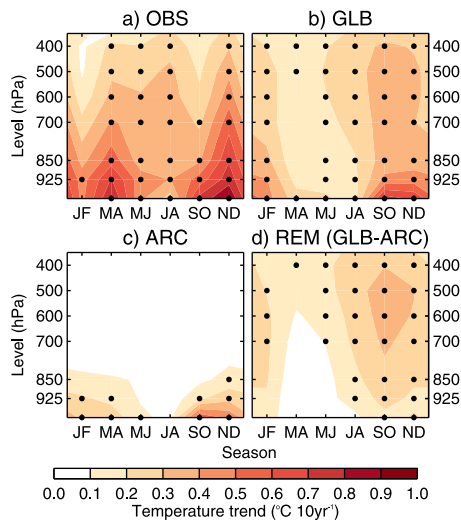


Figure 3. (a) Vertical and seasonal structure of the reanalysis ensemble-mean (OBS) Arctic-mean temperature trends (1979–2008). (b–d) As in Figure 3a, but for the model ensemble-mean trends in the GLB and ARC experiments, and their difference (REM), respectively. Black dots show trends that are statistically significant at the 95% level ($p < 0.05$).

differences can be partially, but not fully, accounted for by AIV, and may additionally reflect model biases in climatological-mean temperature inversion strength and land surface changes that have not been specified.

[20] We now consider the relative contributions of Arctic SIC and SST changes versus non-Arctic SST changes to observed Arctic warming. The former is obtained from ARC ensemble-mean temperature trends (Figure 3c) whereas the latter is estimated by subtracting the ensemble-mean temperature trends in ARC from those in GLB (Figure 3d), referred to hereafter as REM. The warming in ARC occurs almost entirely below 700 hPa and is strongly surface-intensified. This is consistent with the thermal response to Arctic sea ice loss found in other AGCM studies [e.g., Deser et al., 2010; Kumar et al., 2010; Orsolini et al., 2012]. One potential caveat is that the overly-strong surface temperature inversions in the models (Figure S1) may result in ice-loss induced warming that is too shallow compared to reality.

[21] In stark contrast to ARC, the warming in REM is larger aloft than at the surface, with maximum warming located in the mid-troposphere (500–600 hPa). This vertical trend profile closely resembles the temperature anomalies correlated with increased atmospheric poleward heat transport [Alexeev et al., 2005; Graversen et al., 2008; Yang et al., 2010]. ARC and REM show broadly similar seasonal trend patterns, with strongest warming in SO. The weakest warming in ARC is in JA, whereas in REM the smallest trends are found in MA and MJ.

[22] In terms of the maximum trend magnitude at any particular altitude, ARC displays stronger warming trends than REM: maximum Arctic-mean warming rates of 0.5–0.6°C per decade (at the surface in SO) compared to 0.3–0.4°C per decade (in the mid-troposphere in SO). Although the warming in REM is not surface-intensified, Arctic-mean warming trends of greater than 0.1°C per decade are found at the surface during September–February. These are only, however, roughly one

third of the magnitude of the surface warming in ARC during the same seasons.

[23] The annual-mean surface warming in ARC is 0.30°C per decade compared to 0.42 in GLB and 0.60°C per decade in OBS. Thus, Arctic SIC and SST changes account for roughly three quarters of the simulated annual-mean Arctic surface warming and one half of the observed annual-mean Arctic surface warming. The difference between ARC and GLB implies that the remote SST change account for approximately one quarter of the simulated annual-mean surface Arctic warming and one fifth of the observed annual-mean Arctic surface warming. Higher in the atmospheric column, at 500 hPa, the annual-mean Arctic warming is 0.02, 0.26 and 0.25°C per decade in ARC, GLB and OBS, respectively. Thus, remote SST changes account for approximately all the simulated and observed annual-mean mid-tropospheric Arctic warming, although there are differences between the OBS, GLB and REM trends for individual seasons.

[24] Lastly, we turn to the contribution of DRF. Figure 4a shows the Arctic-mean temperature trends in ALL, which are in close correspondence with those in GLB (Figure 3b), but for larger tropospheric warming in ALL during JA. This difference is clearer when the trends in GLB are subtracted from those in ALL, providing an estimate of the component of the trends solely due to DRF (Figure 4b). In JA, DRF is responsible for vertically-uniform Arctic-mean warming of 0.2–0.3°C per decade throughout the free troposphere (i.e., at all levels except the surface). The contribution of DRF is small outside of JA (less than 0.2°C per decade).

4. Discussion and Conclusions

[25] We have quantified the relative contributions of Arctic SIC and SST changes, remote SST changes and DRF to recent Arctic warming. All three forcing factors are important for explaining the observed vertical profile and seasonality of Arctic warming. However, their relative importance differs considerably with altitude and season. Arctic SIC and SST changes are the main driver of near-surface temperature trends, but have had a negligible influence on temperature trends above 700 hPa. By contrast, remote SST changes, and presumably consequent increased poleward energy transport, have been central to the observed warming aloft. Remote SST changes have made a much

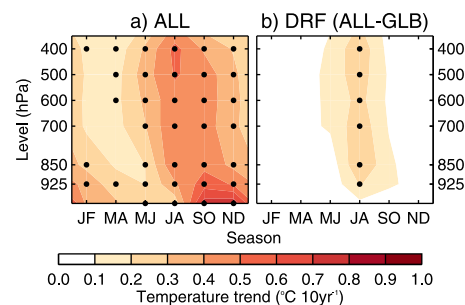


Figure 4. (a) Vertical and seasonal structure of the ensemble-mean Arctic-mean temperature trends (1979–2008) in the ALL experiment. (b) As in Figure 4a, but for difference between the ALL and GLB experiments. Black dots show trends that are statistically significant at the 95% level ($p < 0.05$).

smaller, but non-negligible, contribution to observed near-surface warming trends. DRF has primarily contributed to Arctic tropospheric warming in summer.

[26] Our results demonstrate that the vertical profile of Arctic warming provides insight into the relative importance of the driving mechanisms. Our simulations support the conclusions of *Serreze et al.* [2009] and *Screen and Simmonds* [2010a], that the surface-intensification of recent Arctic warming is evidence of AA due to Arctic sea ice loss (and associated local SST change). Equally, they also provide support for the stance of *Graversen et al.* [2008] and others, that warming aloft is driven by, and therefore indicative of, changes in poleward heat transport.

[27] We close by commenting that this study has not attempted to separate the components of Arctic warming due to anthropogenic forcing (e.g., greenhouse gases, ozone, sulphate aerosols), natural forcing (e.g., solar output, volcanic aerosols) or internal climate (oceanic) variability. On this topic, *Gillett et al.* [2008] concluded that “observed changes in Arctic [and Antarctic] temperatures are not consistent with internal climate variability or natural climate drivers alone, and are directly attributable to human influence”. Based on proxy temperature records (mostly for summer), *Kaufmann et al.* [2009] showed that the 10-year period ending in 2008 was the warmest decade of the past 2000 years in the Arctic. The Arctic is currently in an extraordinary period of warmth.

[28] **Acknowledgments.** The authors thank JMA, ECMWF, NASA and NCEP for providing on-line access to their reanalysis data sets. J. Screen and I. Simmonds acknowledge support from the Australian Research Council. The UM7.3 simulations were supported by an award under the Merit Allocation Scheme on the Australian National Computational Infrastructure. NCAR is sponsored by the National Science Foundation. The CAM3 simulations were kindly provided by R. Tomas and A. Phillips in support of a grant from the NSF Office of Polar Programs awarded to C. Deser. Two anonymous reviewers are thanked for their time and advice.

[29] The editor thanks Chul Chung and an anonymous reviewer for assisting with the evaluation of this paper.

References

- Alexeev, V., P. Langen, and J. Bates (2005), Polar amplification of surface warming on an aquaplanet in ghost forcing experiments without sea ice feedbacks, *Clim. Dyn.*, *24*, 655–666.
- Alexeev, V., I. Esau, I. Polyakov, S. Byam, and S. Sorokina (2012), Vertical structure of recent Arctic warming from observed data and reanalysis products, *Clim. Change*, *111*, 215–239.
- Bintanja, R., R. Graversen, and W. Hazeleger (2011), Arctic winter warming amplified by the thermal inversion and consequent low infrared cooling to space, *Nat. Geosci.*, *4*, 758–761.
- Chung, C. E., and P. Räisänen (2011), Origin of the Arctic warming in climate models, *Geophys. Res. Lett.*, *38*, L21704, doi:10.1029/2011GL049816.
- Collins, W., P. Rasch, B. B. J. Hack, J. McCaa, D. Williamson, B. Briegleb, C. Bitz, S.-J. Lin, and M. Zhang (2006), The formulation and atmospheric simulation of the Community Atmosphere Model Version 3 (CAM3), *J. Clim.*, *19*, 2144–2161.
- Comiso, J. C., C. L. Parkinson, R. Gersten, and L. Stock (2008), Accelerated decline in the Arctic sea ice cover, *Geophys. Res. Lett.*, *35*, L01703, doi:10.1029/2007GL031972.
- Dee, D., et al. (2011), The ERA-Interim reanalysis: Configuration and performance of the data assimilation system, *Q. J. R. Meteorol. Soc.*, *137*, 553–597.
- Déry, S. J., and R. D. Brown (2007), Recent Northern Hemisphere snow cover extent trends and implications for the snow-albedo feedback, *Geophys. Res. Lett.*, *34*, L22504, doi:10.1029/2007GL031474.
- Deser, C., and A. Phillips (2009), Atmospheric circulation trends, 1950–2000: The relative roles of sea surface temperature forcing and direct atmospheric radiative forcing, *J. Clim.*, *22*, 396–413.
- Deser, C., R. Tomas, M. Alexander, and D. Lawrence (2010), The seasonal atmospheric response to projected Arctic sea ice loss in the late twenty-first century, *J. Clim.*, *23*, 333–351.
- Folland, C. K., D. M. H. Sexton, D. J. Karoly, C. E. Johnson, D. P. Rowell, and D. E. Parker (1998), Influences of anthropogenic and oceanic forcing on recent climate change, *Geophys. Res. Lett.*, *25*, 353–356.
- Gillett, N., D. Stone, P. Stott, T. Nozawa, A. Karpechko, G. Hegerl, M. Wehner, and P. Jones (2008), Attribution of polar warming to human influence, *Nat. Geosci.*, *1*, 750–754.
- Graversen, R., T. Mauritsen, M. Tjernström, E. Källén, and G. Svensson (2008), Vertical structure of recent Arctic warming, *Nature*, *451*, 53–56.
- Graversen, R., T. Mauritsen, S. Drijfhout, M. Tjernström, and S. Mårtensson (2011), Warm winds from the Pacific caused extensive Arctic sea-ice melt in summer 2007, *Clim. Dyn.*, *36*, 2103–2112.
- Hurrell, J., J. Hack, D. Shea, J. Caron, and J. Rosinski (2008), A new sea surface temperature and sea ice boundary dataset for the Community Atmosphere Model, *J. Clim.*, *21*, 5145–5153.
- Intergovernmental Panel on Climate Change (2007), *Climate Change 2007: The Physical Science Basis. Contribution of Working Group I to the Fourth Assessment Report of the Intergovernmental Panel on Climate Change*, edited by S. Solomon et al., Cambridge Univ. Press, Cambridge, U. K.
- Kaufmann, D., et al. (2009), Recent warming reverses long-term Arctic cooling, *Science*, *325*, 1236–1239.
- Kumar, A., J. Perlwitz, J. Eischeid, X. Quan, T. Xu, T. Zhang, M. Hoerling, B. Jha, and W. Wang (2010), Contribution of sea ice loss to Arctic amplification, *Geophys. Res. Lett.*, *37*, L21701, doi:10.1029/2010GL045022.
- Lu, J., and M. Cai (2009), Seasonality of polar surface warming amplification in climate simulations, *Geophys. Res. Lett.*, *36*, L16704, doi:10.1029/2009GL040133.
- Martin, G. M., et al. (2011), The HadGEM2 family of Met Office Unified Model climate configurations, *Geosci. Model Dev.*, *4*, 723–757.
- Medeiros, B., C. Deser, R. Tomas, and J. Kay (2011), Arctic inversion strength in climate models, *J. Clim.*, *24*, 4733–4740.
- Meehl, G., et al. (2006), Climate change projections for the twenty-first century and climate change commitment in the CCSM3, *J. Clim.*, *19*, 2597–2616.
- Onogi, K., et al. (2007), The JRA-25 reanalysis, *J. Meteorol. Soc. Jpn.*, *85*, 369–432.
- Orsolini, Y., R. Senan, R. Benestad, and A. Melsom (2012), Autumn atmospheric response to the 2007 low Arctic sea ice extent in coupled ocean–atmosphere hindcasts, *Clim. Dyn.*, doi:10.1007/s00382-011-1169-z, in press.
- Rienecker, M., et al. (2011), MERRA: NASA’s modern-era retrospective analysis for research and applications, *J. Clim.*, *24*, 3624–3648.
- Saha, S., et al. (2010), The NCEP climate forecast system reanalysis, *Bull. Am. Meteorol. Soc.*, *91*, 1015–1057.
- Screen, J., and I. Simmonds (2010a), The central role of diminishing sea ice in recent Arctic temperature amplification, *Nature*, *464*, 1334–1337.
- Screen, J. A., and I. Simmonds (2010b), Increasing fall-winter energy loss from the Arctic Ocean and its role in Arctic temperature amplification, *Geophys. Res. Lett.*, *37*, L16707, doi:10.1029/2010GL044136.
- Screen, J., and I. Simmonds (2011), Erroneous Arctic temperature trends in the ERA-40 reanalysis: A closer look, *J. Clim.*, *24*, 2620–2627.
- Sedláček, J., R. Knutti, O. Martius, and U. Beyerle (2012), Impact of a reduced Arctic sea ice cover on ocean and atmospheric properties, *J. Clim.*, *25*, 307–319.
- Serreze, M., and R. Barry (2011), Processes and impacts of Arctic amplification: A research synthesis, *Global Planet. Change*, *77*, 85–96.
- Serreze, M., and J. Francis (2006), The Arctic amplification debate, *Clim. Change*, *76*, 241–264.
- Serreze, M., A. Barrett, J. Stroeve, D. Kindig, and M. Holland (2009), The emergence of surface-based Arctic amplification, *Cryosphere*, *3*, 11–19.
- Yang, X.-Y., J. C. Fyfe, and G. M. Flato (2010), The role of poleward energy transport in Arctic temperature evolution, *Geophys. Res. Lett.*, *37*, L14803, doi:10.1029/2010GL043934.
- Zhang, Y., D. Siedel, J.-C. Golaz, C. Deser, and R. Tomas (2011), Climatological characteristics of Arctic and Antarctic surface-based inversions, *J. Clim.*, *24*, 5167–5186.